Journal of Simulation & Analysis of Novel Technologies in Mechanical Engineering
10 (4) (2017) 0005~0014
HTTP://JSME.IAUKHSH.AC.IR
ISSN: 2008-4927

Micromachining the Aluminium Tubes Using Abrasive Finishing in Alternating Magnetic Field

Reza Abedinzadeh[1]*, Rasoul Gorji[1]

[1]*Department of Mechanical Engineering, Khomeinishahr Branch, Islamic Azad University, Isfahan, 84175-119, Iran*

(Manuscript Received --- 18 Nov. 2017; Revised --- 03 Jan. 2018; Accepted --- 11 Mar. 2018)

*Corresponding author: abedinzadeh@iaukhsh.ac.ir

Abstract

This study introduced a method based on magnetic field assisted finishing mechanism for micromachining the inner surfaces of Aluminum tubes. In this approach, using the alternating magnetic field of an AC electromotor, abrasive particles were formed as Magnetic Rods (Magnetic Clusters) and surface micromachining was carried out by the dynamic particular pattern made by an alternating magnetic field. The aim of this process was to improve machining efficiency of Aluminum tubes based on surface roughness and dimensional tolerance. Continuously, the effects of parameters such as tube inner diameter, abrasive particles weight, current frequency and machining time on changes of surface roughness were assessed by DOE technique. Taguchi standard orthogonal method (L_9 (3^4)) was used to analyze the process factors. Moreover, the output results derived from experiments were analyzed by two most widely used analytical techniques including Signal to Noise ratio (S/N) and Analysis of Variance (ANOVA). Finally, by considering the results of analysis and plotted graphs, abrasive particles weight and current frequency were identified as significant factors and the optimum conditions of process including tube inner diameter of 55 mm, abrasive particles weight of 1 g, frequency of 40 Hz and machining time of 60 s were obtained.

Keywords: Abrasive finishing, Alternating magnetic, Taguchi, ANOVA, Roughness.

1- Introduction

The parts with high precision finished surfaces are more considerable in the manufacturing companies such as semiconductors, optics, aerospace and precision engineering [1,2]. The defects of workpiece surfaces are resulted from various manufacturing processes. It is difficult to eliminate surface defects in finishing the advanced materials surfaces [3]. Therefore, magnetic field assisted machining processes were recently designed as micromachining process for removing surface defects, increasing workpiece fatigue life and improving surface roughness [4]. In these final machining processes such as magnetic abrasive finishing (MAF), material removal is accomplished by abrasive particles under an applied magnetic field [5,6]. These particles as cutting tools are applied on internal or external faces of materials to enhance the surface properties [7-11].

In recent years, numerical and experimental studies were accomplished to

develop MAF process for technologies such as finishing the free-form surfaces [12, 13]. Jayswal et al. [14] studied theory of MAF process and used finite element modelling to analyze the magnetic forces during finishing process. In this research, a model was proposed for parameters such as surface roughness and material removal. Lin et al. [15] used the DOE technique with Taguchi method to describe the effective parameters on MAF process of stainless steel SUS 304. The surface roughness was improved from primary R_a=2.670 μm to R_a=0.158 μm using MAF process. Jae-Seob Kwak and Tae-Kyung Kwak [16] employed MAF process to finish magnesium plates using magnetic abrasive particles. In their research, DOE technique was used to optimize the effective parameters on surface roughness. Givi et al. [1] performed high level surface machining of aluminum sheet using the rotation of the permanent poles on the back of the aluminum sheet. They studied the effect of parameters such as abrasive particles weight, gap, rotational speed of poles and the finishing cycles on the measured roughness using factorial method. Girma et al. [17] revealed that machining mechanisms of cylindrical and flat surfaces were different. According to their results, obtaining high-quality level in the cylindrical surface is more difficult, requiring more investigation to promote the obtained surface quality by making some changes in this process. Wang and Hu [18] reported that material removal rate is affected by material and size of abrasive particles and finishing speed in MAF process of materials tubing. Kang et al. [19] introduced a high-speed multipolar system and investigated rotational speed effect on machining the capillary tube inner surface. They showed that velocity of 10000 rpm was optimal to obtain improved surface roughness. Despite the advantages of MAF process, it is difficult to finish the flat and micro complex surfaces using this process [20]. The agglomeration of abrasive particles is occurred under direct magnetic field of conventional MAF process. Therefore, the recovery of particles shape is difficult during material removing of surface. In addition, the non-uniformity of finishing process is carried out due to non-uniform distribution of abrasive particles. Furthermore, the cutting edges of particles dulled due to continuous machining process decrease the finishing efficiency.

In this research, we firstly introduced a method based on alternating magnetic field assisted finishing mechanism for micromachining the inner surface of Aluminum tubes. Compared to conventional MAF process, in new MAF process, the fluctuation of abrasive particles during the alternating magnetic field improves surface finishing and increases finishing efficiency. Secondly, the effects of tube inner diameter, abrasive particles weight, current frequency and machining time on the changes of surface roughness (ΔR_a) were studied using DOE technique and the optimal value for each parameter was determined. Improvement in the surface quality with controlled minimum material removal results in keep the dimensional tolerances.

2- Material and methods

2-1- Setup of experiment

As shown in Fig. 1, the setup consists of a stator of AC electromotor, an inverter, and a chuck for clamping the workpiece. The stator generates the requisite alternating magnetic field and the inverter regulates

the rotational speed of the abrasive particles by setting up the input frequency of stator. The experimental conditions are presented in Table 1. In this study, Aluminum AA6063 extruded tube and steel grits were used as workpiece and abrasive particles, respectively.

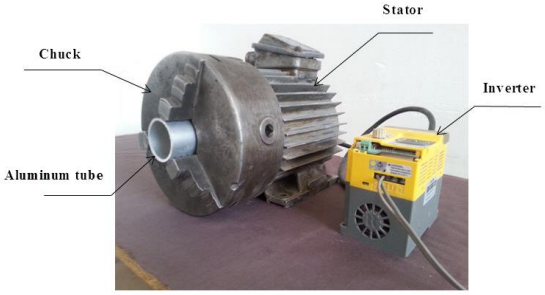

Fig. 1. The experimental setup for polishing of Aluminum tube.

Table 1. Details of experimental conditions and materials.

Stator	1.1 kW, Cos φ*= 0.88, 2890 rpm, 50 Hz, 2.3/4 A, Internal diameter 80 mm
Inverter	RHYMEBUS, RM5E-2002
Aluminum tube	AA6063, Length 300 mm, Primary roughness 0.3-0.8 µm
Abrasive particles	Steel, Hardness 50-60 HRC, Density 7g/cm^3, Mesh size 0.125-0.3 mm, Chemical detail: Carbon 0.85-1.2%, Silicon 0.40%, Manganese 0.60-1.20%, Sulfur 0.05%MAX, Phosphorus 0.05%MAX

* Cos φ: Power factor for an AC electromotor and φ: phase angle between voltage and current.

2-2- Material removal mechanism in finishing the inner surface of a tube

2-2-1- Magnetic abrasive motion

In the proposed MAF process, Aluminum tube with abrasive particles was concentrically placed inside the stator of AC electromotor (Fig. 2). Subsequently, the magnetic field was created in the coil of stator (windings) using an applied current, and the formation of abrasive particles along the magnetic field, called Magnetic Rods (MRs) or Magnetic Clusters, was accomplished under the generated magnetic field (Fig. 3). These MRs were placed along the new magnetic field by changing the current from a coil to an adjacent coil. Therefore, MRs had two kinds of motion including the rotation around their axis, parallel to the axis of the tube, and rotation around circumference of tube inner surface. Most material removal is performed in both edges of MRs due to the combination of the above two motions. The length of MRs due to fluctuation up and down in alternating magnetic field, is various; thus, abrasive machining at different points is carried out randomly. This can be led to increase the surface quality.

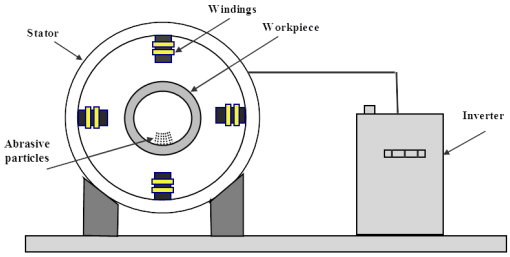

Fig. 2. Schematic of MAF process for finishing of tube inner surface.

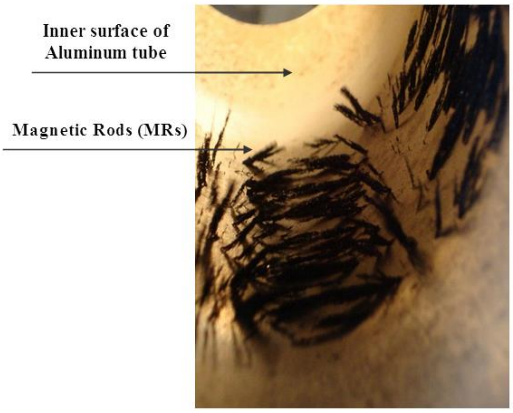

Fig. 3. Formation of Magnetic Rods (MRs) inside the Aluminium tube, at the beginning process with low frequency.

2-2-2- Force analysis of an abrasive particle on inner surface of a tube

A schematic view of applied forces to an abrasive particle during finishing process the internal surface of a tube is shown in Fig. 4. The magnetic force (F) applying to

the abrasive particle is expressed as in (1) [21]:

$$F=\sqrt{F_x^2+F_y^2}$$
$$F_x=\frac{\pi d^3}{6}\frac{\chi}{(1+\chi)^2\mu_0}\left(\frac{\partial B}{\partial x}\right) \quad (1)$$
$$F_y=\frac{\pi d^3}{6}\frac{\chi}{(1+\chi)^2\mu_0}\left(\frac{\partial B}{\partial y}\right)$$

where d is the abrasive particle diameter, χ is particle magnetization susceptibility, μ_0 is vacuum permeability, B is the strength of magnetic field, $\frac{\partial B}{\partial x}$ and $\frac{\partial B}{\partial y}$ and are magnetic field gradients in x and y directions. The centrifugal force (F_c) is also calculated, as shown in (2):

$$F_c=m(D-d)\omega^2/2 \quad (2)$$

where D is the tube internal radius, m is abrasive particle mass and ω is angular velocity of an abrasive particle. The normal force (F_n) and tangential force (F_t) are calculated as in (3):

$$F_n=F\cos\beta+mg\cos\alpha+m(D-d)\omega^2/2 \quad (3)$$
$$F_t=F\sin\beta+mg\sin\alpha$$

According to Fig. 4, normal magnetic force penetrates abrasive particles into the tube surface and tangential magnetic force leads to generate an abrasive particle movement against the workpiece surface which results in material removal like micro-chip [19].

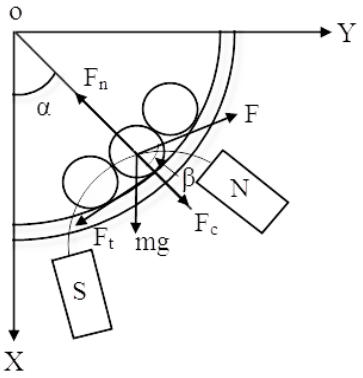

Fig. 4. The applied forces to an abrasive particle during abrasive finishing process [21].

2-3- Experimental procedure

Experiment tests were performed to assess the effective parameters including tube inner diameter, abrasive particles weight, current frequency and machining time on the surface roughness changes as an output parameter (ΔR_a). In order to improve the measured parameters, tubes were firstly cut into two parts and roughness was measured at two points of inner surface using the roughness tester (Mahr Set M300-RD18). Then, the parts were joined together and placed in MAF apparatus. By clamping the tube in the chuck, tube and stator became coaxial. Abrasive particles were weighed with the accuracy of 0.001 g and added into the tube. Subsequently, the desired frequency was adjusted using the inverter and machining time was measured. For any test, the measurement of surface roughness was carried out at two marked points and the amount of ΔR_a for any point was obtained.

2-4- Design of experimental technique

In this research, Taguchi standard orthogonal method was used to evaluate four parameters including tube inner diameter, abrasive particles weight, frequency and machining time. Each parameter as variable factor was defined in three levels (Table 2). Using the Taguchi method, the number of 3^4=81 tests was substituted by optimal nine experiments to decrease the calculation time (Table 3). Reducing the number of experiments is performed using the special design of orthogonal array in this method. Also, the analysis of the acquired data from this method was simpler in comparison with other methods [22]. The Signal to Noise ratio (S/N) technique was used to analyze

the obtained results and illustrate the optimum conditions. Significance of parameters was also studied by ANOVA method.

Table 2. Input parameters as variable factors used for Design of Experiment technique with Taguchi orthogonal standard method L_9 (3^4).

Parameters	Factor	Type	Levels	Value
Tube inner diameter (mm)	C1	fixed	3	30, 45, 55
Abrasive particles weight (g)	C2	fixed	3	1, 5, 9
Frequency (Hz)	C3	fixed	3	20, 30, 40
Machining time (s)	C4	fixed	3	30, 60, 90
Roughness changing (µm)	C5	-	-	-

2-5- Data analysis

Optimizing technique was carried out using the Taguchi and Analysis of Variance (ANOVA) methods in analytical SPSS software. Also, the accuracy of experiments was investigated by depicting various diagrams.

2-5-1- Signal to Noise ratio (S/N)

Optimizing technique with Taguchi method was performed using Signal to Noise ratio (S/N) method to obtain the optimal conditions among experiments. After analyzing with S/N method, the best level was introduced for any factor.

Table 3. Design of experiments with Taguchi orthogonal standard method L_9 (3^4), ΔR_{a1}, ΔR_{a2} and calculated η for nine tests.

	Tube inner diameter (mm)	Abrasive particle Weight (g)	Frequency (Hz)	Machining Time (s)	ΔR_{a1} (µm)	ΔR_{a2} (µm)	ŋ
1	30	1	20	30	0.129	0.102	18.689
2	30	5	30	60	0.088	0.122	19.463
3	30	9	40	90	0.051	0.047	26.188
4	45	1	30	90	0.079	0.005	25.040
5	45	5	40	30	0.075	0.082	22.094
6	45	9	20	60	0.065	0.067	23.608
7	55	1	40	60	0.036	0.016	31.101
8	55	5	20	90	0.269	0.102	13.831
9	55	9	30	30	0.041	0.038	28.061

The main idea in S/N analyzing is that in the optimal conditions, performance variability in response to noises becomes minimal. On the other hand, there are optimal conditions under which changes in output values become more dependent on signal values than noise values [23].Therefore, S/N analysis specifies optimal conditions in cases with maximum signal to noise ratio. The aim of this study was to decrease ΔR_a for improving surface roughness and keeping dimensional tolerances. Thus, Smaller the Better (SBT) state was chosen. η, as the analyzing parameter of S/N method in SBT state, is calculated as in (4):

$$\eta = -10\log_{10}\left[\frac{1}{n}\sum_{i=1}^{n} y_i^2\right] \quad (4)$$

where y_i is the respective output of i_{th} test and n is repeat cycles number. Thus, η for any experiment related to identify a series of control factors settings is calculable. Among η values, the larger value shows the optimal conditions. As shown in Table 3, maximum value η was obtained in experimental test 7, which described how the parameters were optimized in this test. According to main effects plot (Fig. 5), the maximum value in this diagram was the optimal value. Therefore, tube inner diameter of 55 mm, abrasive particles weight of 1 g, frequency of 40 Hz and machining time of 60 s were optimal values in these tests.

2-5-2- Analysis of Variance

The analysis of variance technique is used for covering the inadequacy of graphical assessments. The use of this method can clarify significant parameters and their effects on the process. On the other hand, while a parameter is significant, it has a remarkable effect on the process and insignificance of a parameter shows the negligible effect of the parameter in the process. Significant level was defined as P=0.05 in the analysis and the parameter was significant for an amount lower than 0.05. Table 4 shows that both parameters of frequency and abrasive particles weight are significant. It is notable that both parameters of tube inner diameter and machining time are also effective in the process, but their effect is negligible. According to Table 4, the values of R^2 (R-Sq) and total error squares (S) parameters were 69.29% and 0.0445, respectively which indicates a good fit linear model for ΔR_a.

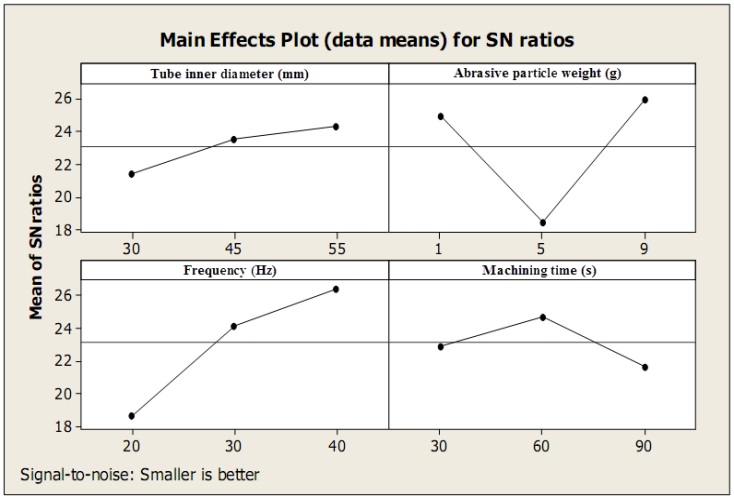

Fig. 5. Main effects plot in S/N method.

Table 4. The data resulting from analysis of variance technique for ΔR_a.

Source	DF	Seq SS	Adjusted SS	Adjusted MS	F	P
C1	2	0.002531	0.002531	0.001266	0.64	0.551
C2	2	0.018058	0.018058	0.009029	4.55	0.043
C3	2	0.017611	0.017611	0.008806	4.44	0.046
C4	2	0.002111	0.002111	0.001056	0.53	0.605
Error	9	0.017864	0.017864	0.001985	0.64	0.551
Total	17	0.058176	-	-	-	-

In Fig. 6, the residual analysis plots for ΔR_a are depicted. Plot of normal probability for residuals is in relation to data validation (Fig. 6a). In general, if all points tend to form a line, it means a normal distribution of the residuals. In this experiment, the points were relatively placed on a line which means that the experimental outputs are approximately normal. However, in this experiment, due to the use of the DOE technique with Taguchi standard method, the normal factor was not much important. The residuals versus the fitted values plot demonstrates the convergence and outputs normality (Fig. 6b). As shown, the residuals exhibited a random pattern around zero line which demonstrates the variance constancy [1].

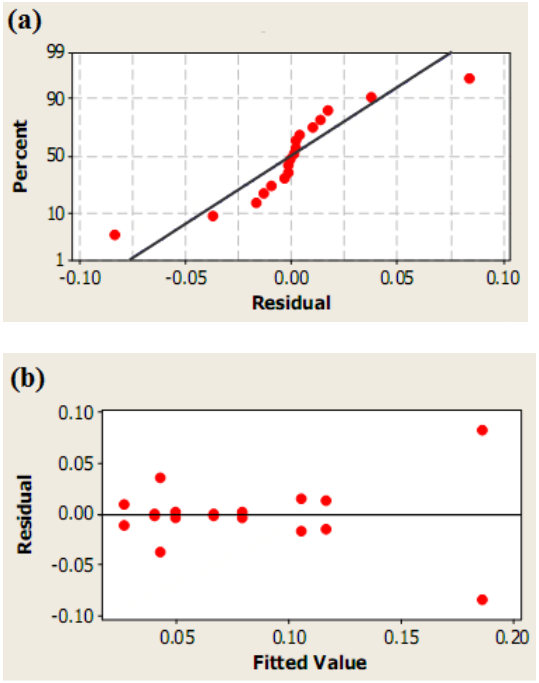

Fig. 6. (a) Plot of normal probability and (b) plot of residuals versus the fitted values.

3- Results and discussion

The effective process parameters on the surface roughness changes are shown in Fig. 7. According to this figure, the effects of input parameters including tube inner diameter, abrasive particles weight, frequency and machining time on the output parameter ΔR_a were investigated as follows.

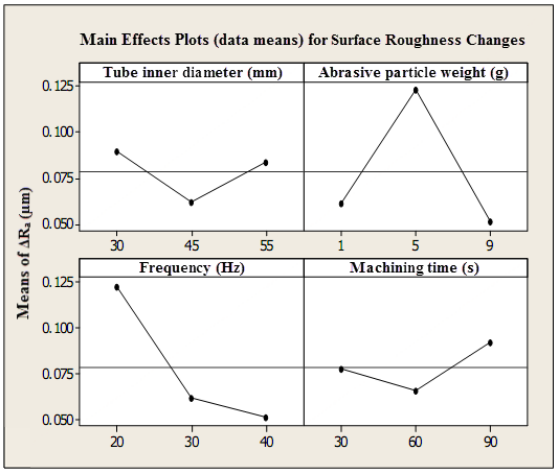

Fig. 7. The effective process parameters on the surface roughness changes (ΔR_a) using ANOVA method.

3-1- Effect of tube inner diameter

According to Fig. 7, it was observed that with increasing the tube inner diameter to the inner diameter of the stator (80 mm), ΔR_a was initially decreased and then increased. In the range of 45 mm to 55 mm, ΔR_a is increased with increasing the tube diameter. According to Eqs. (2) and (3), an increase in tube diameter results in increasing the centrifugal force (F_c). Therefore, the abrasive particles exhibit more pressures into the inner surface of tube using an increased normal magnetic force. Also, when tube diameter is large and close to the inner diameter of stator, there are parallel magnetic field lines which are perpendicular to the workpiece surface. Thus, an increase in MRs formation is carried out by a high intensity magnetic field. According to Eqs. (1) and (3), the higher magnetic force (F) pushes the MRs into surface. Thus, the material

removal and surface roughness changes are increased. However, it is observed that with reducing the diameter to 30 mm, ΔR_a was increased that exhibits a different behavior. Due to the oblique magnetic field lines and lower magnetic flux density in the small diameters, a reduction in MRs formation can be occurred. Therefore, the length of MRs is greatly decreased and the number of MRs with cutting edges is increased. This can be led to increase material removal and surface roughness changes.

3-2- Effect of abrasive particles weight

As shown in Fig. 7, ΔR_a is smaller in lower particles weight, because MRs are not formed sufficiently to remove material. It is observed that ΔR_a increases when abrasive particles weight increases to 5 g. In fact, the particles contributing in the abrasive machining process are increased. The centrifugal force (F_c) are also increased with increasing the abrasive particle weight. This factor has influence on the normal cutting force. However, when abrasive particles weight is increased to 9 g, accumulation of the particles in the tube is occurred and the magnetic field distribution is conducted to more particles. This leads to reduce the amount of material removal and changes of surface roughness. The particle weight effect on changes of surface roughness was also reported by Gandhi and Singh [24].

3-3- Effect of frequency

According to Fig. 7, ΔR_a decreases with increasing the frequency to 40 Hz. This means that increasing the frequency exhibits fewer effects on the magnetic force during finishing process. The current frequency affects the angle of magnetic particles (θ), as shown in Fig. 8. In the condition of lower frequency, the angle of MRs change is greater [20]. This results in more flexibility of MRs. This can be resulted that increasing the MRs angle variation leads to enhance the cross-cutting effects of MRs. Thus, more material removal is performed by MRs and ΔR_a is increased.

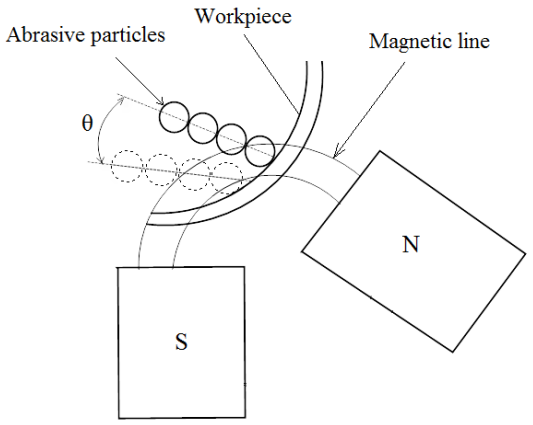

Fig. 8. abrasive particles movement in alternating magnetic field.

3-4- Effect of machining time

According to Fig. 7, ΔR_a decreases with increasing the machining time from 30 s to 60 s and then increases in the range of 60 s to 90 s. In the range of 30 s to 60 s, smooth surface is obtained by removing the peaks by MRs and ΔR_a reaches to lower value (0.016 μm). After machining time of 60 s, due to the low surface roughness, in addition to peaks removal, the valleys are removed by MRs and ΔR_a is increased. According to the results, optimum machining time is 60 s which is similar to results of S/N analysis. However, this parameter is not significant and its changes have no significant effect on the process.

4- Conclusions

In this paper, micromachining the inner surface of Aluminum tubes was

accomplished using abrasive finishing process in alternating magnetic field. Moreover, DOE technique was used to investigate the effective parameters on the surface roughness changes. The aim of this research was to improve the efficiency in the micromachining operations regarding to surface roughness and dimensional tolerance factors. The following results can be summarized in this study:

1. By using the S/N method, optimal values of the parameters including tube inner diameter of 55 mm, abrasive particles weight of 1 g, frequency of 40 Hz, and machining time of 60 s were obtained.

2. Abrasive particles weight and frequency with P values of 0.043 and 0.046 respectively, were identified as the effective controllable parameters on the process using the ANOVA method.

3. The surface roughness changes and material removal increase generally with increasing the tube inner diameter, abrasive particle weight and machining time.

4. It seems that at higher frequencies, the tolerances were maintained with more accuracy by considering the lower value of ΔR_a.

References

[1] M. Givi, A.F. Tehrani, and A. Mohammadi, "Polishing of the aluminum sheets with magnetic abrasive finishing method," *Int. J. Adv. Manuf. Tech.*, vol. 61, pp. 989-98, 2012.

[2] V. Grover, and A.K. Singh, "A novel magnetorheological honing process for nano-finishing of variable cylindrical internal surfaces," *Mater. Manuf. Process.*, vol. 32, pp. 573-580, 2017.

[3] A. Manna, and A. Kundal, "Micro machining of nonconductive Al_2O_3 ceramic on developed TW-ECSM setup," *Int. J. Manuf. Mater. Mech. Eng.*, vol. 1, pp. 46-55, 2011.

[4] K. Rakhimyanov, and I. Semenova, "Surface state control by ultrasonic plastic deformation at the final machining stage," *Mater. Manuf. Process.*, vol. 31, pp. 764-9, 2016.

[5] P. Saraeian, H. Soleimani Mehr, B. Moradi, H. Tavakoli, and O. Khalil Alrahmani, "Study of magnetic abrasive finishing for AISI321 stainless steel," *Mater. Manuf. Process.*, vol. 31, pp. 2023-9, 2016.

[6] C. Vipin, and M. Shukla & Pulak, "Experimental investigations into sintering of magnetic abrasive powder for ultrasonic assisted magnetic abrasive finishing process," *Mater. Manuf. Process.*, vol. 32, pp. 108-14, 2017.

[7] G. Singh, A.K. Singh, and P. Garg, "Development of Magnetorheological finishing process for external cylindrical surfaces," *Mater. Manuf. Process.*, vol. 32, pp. 581-8, 2017.

[8] M. Sushil, K. Vinod, and K. Harmesh, "Experimental investigation and optimization of process parameters of Al/SiC MMCs finished by abrasive flow machining," *Mater. Manuf. Process.*, vol. 30, pp. 902-11, 2015.

[9] N. Francis, K. Viswanadhan, and M. Paulose, "Swirling abrasive fluidized bed machining: Effect of process parameters on machining performance," *Mater. Manuf. Process.*, vol. 30, pp. 852-7, 2015.

[10] J. Sheikh-Ahmad, and J. Mohammed, "Optimization of process parameters in diamond abrasive machining of carbon

fiber-reinforced epoxy," *Mater. Manuf. Process.*, vol. 29, pp. 1361-6, 2014.

[11] R. Ferreira, D. Carou, C. Lauro, and J. Davim, "Surface roughness investigation in the hard turning of steel using ceramic tools," *Mater. Manuf. Process.*, vol. 31, pp. 648-52, 2016.

[12] S.M. Ji, Y.M. Xu, G.D. Chen, and M.S. Jin, "Comparative study of magnetic abrasive finishing in free-form surface based on different polishing head," *Mater. Sci. Forum*, vol. 675, pp. 593-596, 2011.

[13] K. Judal, and V. Yadava, "Modeling and simulation of cylindrical electrochemical magnetic abrasive machining process," *Mach. Sci. Technol.*, vol. 18, pp. 221-50, 2014.

[14] S. Jayswal, V. Jain, and P. Dixit, "Modeling and simulation of magnetic abrasive finishing process," *Int. J. Adv. Manuf. Tech.*, vol. 26, pp. 477-90, 2005.

[15] C.T. Lin, L.D. Yang, and H.M. Chow, "Study of magnetic abrasive finishing in free-form surface operations using the Taguchi method," *Int. J. Adv. Manuf. Tech.*, vol. 34, pp. 122-30, 2007.

[16] J. Kwak, and T. Kwak, "Parameter optimization in magnetic abrasive polishing for magnesium plate," *2nd Int. Conf. Comput. Eng. Technol.*, vol. 5, pp. 544-547, 2010.

[17] B. Girma, S.S. Joshi, M. Raghuram, and R. Balasubramaniam, "An experimental analysis of magnetic abrasives finishing of plane surfaces," *Mach. Sci. Technol.*, vol. 10, pp. 323-40, 2006.

[18] Y. Wang, and D. Hu, "Study on the inner surface finishing of tubing by magnetic abrasive finishing," *Int. J. Mach. Tools Manuf.*, vol. 45, pp. 43-9, 2005.

[19] P.S. Kang, L. Singh, and J.S. Gill, "Finishing of SUS 304 stainless steel bent tubes using magnetic abrasive finishing," *Mechanica. Confab. Int. J.*, vol. 2, pp. 123-30, 2013.

[20] J. Wu, Y. Zou, and H. Sugiyama, "Study on finishing characteristics of magnetic abrasive finishing process using low-frequency alternating magnetic field," *Int. J. Adv. Manuf. Tech.*, vol. 85, pp. 585-94, 2016.

[21] X.G. Yao, Y.H. Ding, G. Ya, W.W. Liu, and Y. Zhang, "Study of finishing mechanism for internal surface using magnetic force generated by rotating magnetic field," *Key Eng. Mat.*, vol. 416, pp. 406-410, 2009.

[22] D.C. Montgomery, Design and analysis of experiments; John Wiley & Sons, 2017.

[23] S. Ahmad, S. Gangwar, P.C. Yadav, and D. Singh, "Optimization of process parameters affecting surface roughness in magnetic abrasive finishing process," *Mater. Manuf. Process.*, pp. 1-7, 2017.

[24] G.S. Gandhi, and L. Singh, "Internal finishing of thick cylinder SUS 304 steel tubes using magnetic abrasive finishing setup," *Int. J. Mech. Civil Eng.*, vol. 2, 2013.